

The following publication Hu, E., Wu, X., Shang, S., Tao, X.-M., Jiang, S.-X., & Gan, L. (2016). Catalytic ozonation of simulated textile dyeing wastewater using mesoporous carbon aerogel supported copper oxide catalyst. *Journal of Cleaner Production* 112(Part 5), pp. 4710–4718 is available at <https://doi.org/10.1016/j.jclepro.2015.06.127>.

**Catalytic ozonation of simulated textile dyeing wastewater using mesoporous
carbon aerogel supported copper oxide catalyst**

Enling Hu, Xinbo Wu, Songmin Shang *, Xiao-ming Tao, Shou-xiang Jiang

Institute of Textiles and Clothing, The Hong Kong Polytechnic University, Hong Kong

***Corresponding author:**

Dr. Songmin Shang

Institute of Textiles and Clothing,

The Hong Kong Polytechnic University,

Hong Kong

Tel: +852-34003085

Fax: +852-27731432

E-mail: shang.songmin@polyu.edu.hk

Abstract

Textile dyeing uses large amount of freshwater and synthetic dyes. Its effluents have to be subjected to certain treatments to remove the contaminants, especially for residue dyestuffs, before discharging to water bodies for elimination of adverse impacts to the environment. The objective of this research is to fabricate a novel catalyst, carbon aerogel supported copper oxide, and study its catalytic performance for the first time in ozonation of simulated dyeing wastewater for dye degradation. The catalyst was prepared using sol-gel and impregnation method, and characterized by Transmission Electron Microscope and X-Ray Diffraction techniques which suggesting that the nano-sized copper oxide particles successfully embedded and well-dispersed in the amorphous carbon aerogel. The catalytic performance of the catalyst was evaluated by degradation of C.I. Reactive Black 5 in a semi-continuous reactor. The results show that the catalyst has promising potential in ozonation towards dye elimination in dyeing wastewater, in which the dye removal efficiency can be effectively enhanced by the catalyst. In the specific conditions, COD removal could reach 46% in catalytic ozonation system after 60-min reaction, while it was only 29% in ozonation alone without catalyst. In addition, a systematic parameter study was performed to investigate the effect of the temperature, pH, ozone dosage, catalyst amount and dye concentration on dye degradation in terms of color and COD removal.

Keywords: Wastewater Reactive dye Carbon aerogel Copper oxide Ozonation

1. Introduction

Synthetic dyes are frequently used in the textile dyeing plant for aesthetic consideration of the products. In the dyeing process considerable amount of color effluents of high polluting degree are generated (Asghar et al., 2015), which will adversely influence not only the environment but also human health if it is discharged without adequate treatment (Bootharaju and Pradeep, 2013; Ozturk et al., 2015). In particular, some dyes have toxic, carcinogenic and even genotoxic effects on the humans (Saroj et al., 2014). Thus it is important to remove dyes in the textile wastewater before discharging to receiving water bodies (Wang et al., 2013b). However the removal of different dyes is always a remarkable challenge (Tian et al., 2013). The conventional biological method, which is effective for contaminants removal from municipal sewage, is however not particularly useful for treating textile dyeing wastewater due to low biodegradability of textile dyes. Although many studies show that the removal of textile dyes in effluent by specific natural clays via adsorption is effective and cost-competitive (Abidi et al., 2015), the replacement burden of the adsorbent, which is saturated to dyes after certain service time, has to be carefully evaluated in real wastewater treatment. Chemical oxidation is an effective method to treat textile wastewater by using several active oxidants including chlorine/chlorine dioxide (Vacchi et al., 2013), hydrogen peroxide (Ramachandran and Kumarasamy, 2013) and ozone (He et al., 2013). Particularly, ozone has outstanding oxidizing ability and can decompose to O₂ without byproducts in the whole oxidation process, which therefore has aroused the interests in water/wastewater treatment. The widely accepted theory in ozonation is that there are two reaction pathways in water, the direct and indirect reaction routes. The principle of direct reaction is molecular ozone reacts with organic contaminants, whereas in indirect reaction organic pollutants are oxidized by highly reactive free radicals which derives from decomposition of molecular ozone (Fanchiang and Tseng, 2009). Nonetheless, only partial mineralization of dye compounds could be realized by ozonation (Yıldırım

et al., 2011) and the high energy demand for ozone generation further limits its practical application in wastewater treatment (Mehrjouei et al., 2014). To improve the treatment efficiency and utilization of ozone, several new processes have been developed for degradation of dyes or similar organic compounds, including UV/ O₃/H₂O₂ (Vijayalakshmi et al., 2011), TiO₂/UV/O₃ (Sun et al., 2013b), O₃/H₂O₂ and catalytic ozonation in the presence of certain catalyst (Mahmoodi, 2013; Qiang et al., 2013; Qu et al., 2015).

The heterogenous catalytic ozonation, in which the catalyst is of solid form, has received widely attention in removal of organic pollutants from aqueous solution because of its high efficiency and ambient operational conditions, which has potential practical applications in real water/wastewater treatment without any additional means such as thermal and light energy or second pollution involving ionic catalyst separation in homogenous ozonation. In the past decades, various materials based on transition oxides such as manganese oxide (Zhao et al., 2014), titanium oxide (Yang et al., 2007), zinc oxide (Gharbani and Mehrizad, 2014), nickel oxide (Qin et al., 2009; Zhang et al., 2009), copper oxide (Petre et al., 2013), cerium oxide and iron oxide (Beltran et al., 2005; Ciccotti et al., 2015) were frequently used as ozonation catalysts. The ozone/catalyst process is more efficient than the ozone process alone because these catalysts act as a radical promoter and support (Zhao et al., 2014). Among these, copper oxide has been found to be a promising catalyst because it could increase the reaction rate and diminish the ozone consumption which led to an advanced degradation of organic pollutants (Turkay et al., 2014; Udrea and Bradu, 2003). Moreover, copper oxide has numerous advantages such as cost-competitive, chemically stable and non-toxic. However, a key issue associated with using micro- and nano-sized copper oxide powders for water treatment is the fact that they are difficult to be separated from treated water. In addition, the catalytic efficiency and the stability of catalysts have to be enhanced. These disadvantages restrict the application of powdered catalyst in wastewater treatment.

Recently a novel material, carbon aerogel (CA), has been fabricated as functional materials due to its unique properties which originates from excellent three-dimensional continuous porous structure including great mesopore volume, high surface areas, low mass densities, and good adsorption capacity (Yin et al., 2014; Zhang et al., 2014). It

has been developed for several applications, such as catalyst for decomposition of 4-phenoxyphenol (Park et al., 2013), supercapacitors (Liu et al., 2015a, 2015b), amperometric biosensor (Peng et al., 2015), absorbent for dye removal (Wu et al., 2012), photocatalyst for dye degradation (Lin and Chang, 2014), and electrode for dye decolorization in electrolysis (Wu et al., 2008). With this in mind, the scope of the present paper is to fabricate the novel nano-sized copper oxide catalyst supported on mesoporous carbon aerogel (MCA) and study its catalytic performance in ozonation of simulated dyeing wastewater for dye degradation. The combination of copper oxide and carbon aerogel are likely to exert durable and effective influence in activating O₃ to generate more •OH in the catalytic ozonation synergistically. Furthermore, the introduction of MCA support provides an effective and convenient approach to avoid the disturbing issue in separation of catalyst powder from the treated water after the treatment process (Sun et al., 2013a). Considering more than 50% of cotton is dyed with reactive dyes, which is the most commonly used substrate in dyed textile fibers (Rosa et al., 2015), the water soluble reactive dye, C.I. Reactive Black 5 (RB-5), was hence chosen as the dye pollutant in the present study. The designed catalyst would be prepared by sol-gel polymerization and impregnation method, and characterized by Transmission Electron Microscope (TEM) and X-Ray Diffraction (XRD). The catalyst then would be used in a catalytic ozonation reactor which filled with dye solution and continuously injected with ozone/oxygen gas mixture. Considering some physical and chemical variables may determine the amount of active surface sites of the catalyst, which affects the heterogenous catalytic activity (Woan et al., 2009), the experimental conditions, such as treating time, temperature, working pH, ozone dosage, catalyst dosage and initial dye concentration, would be investigated to confirm their effects on the catalytic behavior of the catalyst in dye elimination. On the basis of literature review, this is the first work involving MCA based material as catalyst for ozonation.

2. Material and methods

2.1. Dye and chemicals

Commercial reactive dye, RB-5 (Chemical formula: C₂₆H₂₁N₅Na₄O₁₉S₆; molecular weight: 991.82 g/mol; λ_{max}: 594 nm), was obtained from Zhejiang Longsheng Group Co., Ltd. and used without further purification. Dye was dried at 378 K in a vacuum

oven for 3 h to remove water before use. The simulated dyeing wastewater were prepared by dissolving 3.2 g of RB-5 dye in a 1 L volumetric flask (3200 mg/L) firstly, and then diluted to a desired concentration with distilled water. Formaldehyde (VWR International), resorcinol (Sigma-Aldrich), Hexadecyl trimethyl ammonium bromide (Alfa Aesar), copper(II) nitrate trihydrate (Sigma-Aldrich) were of analytical grade and used as received.

2.2. Preparation and characteristic of catalyst

MCA was synthesized via sol-gel method (Wu et al., 2007, 2008) and CuO-Cu₂O/MCA was prepared by the impregnation approach (Gomez et al., 2015). To begin with, resorcinol, hexadecyl trimethyl ammonium bromide (HTAB) and formaldehyde (the molar ratios of resorcinol/HTAB and resorcinol/formaldehyde were 125 and 0.5) were dissolved in distilled water at ambient condition (temperature= 24 ± 1 °C, relative humidity= 65 ± 3%). The solution mixture was then poured into a glass bottle and aged at 80 °C for 7 d. Thereafter, the obtained gel, which converted from the solution mixture after ageing, was exposed to air in fume hood to release residual unreacted volatile chemicals at room temperature for 2 d. Subsequently, the sample was dried at 60 °C for 24 h and further dried at 105 °C for 24 h. Finally, MCA was obtained by carbonization in a tube furnace (MTF 12/38/250, Carbolite, UK) at 900 °C for 3 h under Ar gas flow. Before used as the support for nano-sized CuO-Cu₂O catalyst, MCA was crashed into granular form (10-20 mesh) to facilitate impregnation. In impregnation process, dry MCA granules were immersed into 0.2 M Cu(NO₃)₂•3H₂O aqueous solution in an Erlenmeyer flask, which was then mounted into an isothermal waterbath shaker (120 rpm) at 30 °C for 24 h. Later on the soaked granular sample was dried at 60 °C for 24 h first, followed by drying at 105 °C for 6 h. The CuO-Cu₂O/MCA catalyst was then successfully prepared by calcination of the impregnated sample at 450 °C for 4 h.

2.3. Experimental set-up and procedure

Catalytic ozonation was performed in a glass reactor filled with 250 mL of dye solution, of which the temperature and stirring speed were controlled by a Digital Magnetic Hotplate Stirrer (MS- H-Pro, DragonLab's). Fig. 1 shows the schematic of the experimental set-up. Ozone was generated by a high precision medical ozone generator (Medozons BM-02, Russia) fed with oxygen (99.9%, industrial grade, Portapak)

provided by Linde HKO Ltd, HK. The mixture gas stream, comprising of ozone and oxygen, was continuously fed into the reaction system through a porous diffuser, which laid at the bottom of the glass reactor for generation of fine bubbles. Solution pH was not adjusted unless indicated in purpose and the off-gas containing residual ozone was adsorbed by potassium iodide solution in two gas washing bottles. At each predetermined time intervals during ozonation, 3 mL of water sample was carefully pipetted from the reactor and diluted appropriately before centrifuged (6000 rpm for 10 min) in a centrifuge (K3 Centurion Scientific Ltd., UK) to settle down the suspended catalyst small particles. The supernatant was then be used for color or COD determination. Each measurement was independently conducted thrice to reduce error, and the average value was accepted.

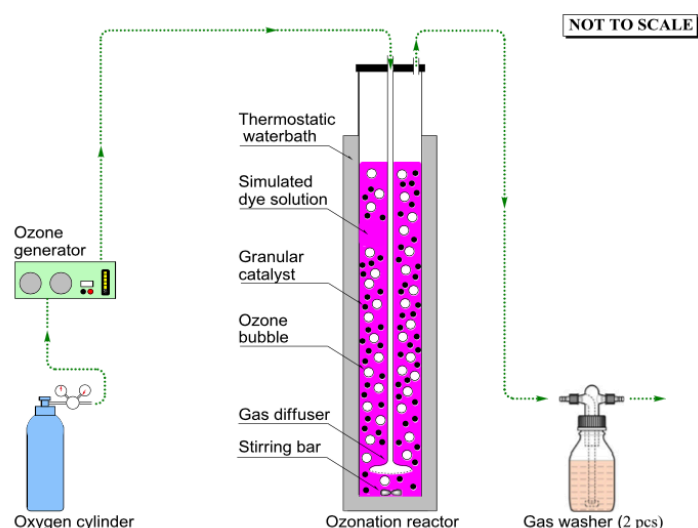


Fig. 1. Experimental set-up for ozonation.

2.4. Analytical method

The structure and morphology of the prepared CuO-Cu₂O /MCA catalyst was investigated by Transmission Electron Microscope (TEM) (JEOL Model JEM-2100F) and Powder X-ray diffraction (XRD) patterns were obtained from a diffractometer (Rigaku, SmartLab) using Cu K α radiation. The degradation efficiency of dye during

catalytic ozonation was determined by the color removal and COD reduction. Color removal was converted from the absorbance, which was measured by a UV-Vis spectrophotometer (PerkinElmer, Lambda 18) at the maximum absorbance wavelength, $\lambda_{\text{max}}= 594 \text{ nm}$, of the dye solution. The COD was determined by the COD colorimeter (Model DR 900, HACH, USA) according to Hach Method 8000. In brief, 2 mL of water sample was added into a COD digestion vial, which was prefilled with 2 mL of essential reagents mixture, followed by heated at 150 °C for 2 h in the digital reactor block (Model DRB 200, HACH, USA). After cooling down to room temperature, the vial was transferred into the COD colorimeter for COD determination.

3. Results and discussion

3.1. Characteristic of catalyst

The XRD patterns of MCA and MCA supported copper oxide (CuO-Cu₂O) presents in Fig. 2. The broad peak at around $2\theta= 23^\circ$ associated to the amorphous structure of carbon material, which is similar to that of carbon nanofiber (Wang et al., 2013a). The diffraction pattern of the prepared samples shows that the copper oxide mainly exists as CuO and Cu₂O. The characteristic peaks at 35.8° and 38.6° were assigned to the (111) and (200) reflections of CuO (JCPDS card No. 65-2309) and those at 36.5°, 42.4° and 61.6° are assigned to the (111), (200) and (220) reflections of Cu₂O (JCPDS card No. 65-3288). Some diffraction peaks of CuO or Cu₂O didn't display in Fig. 2 because the mass proportion of CuO-Cu₂O particles in CuO-Cu₂O /MCA catalyst was minimal and their spectrum signals were therefore weak and apt to be covered by that from MCA.

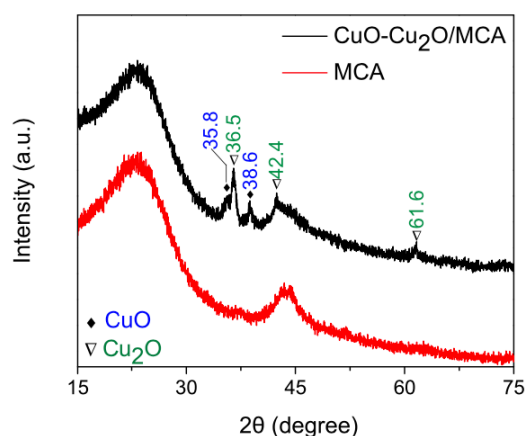


Fig. 2. XRD pattern of MCA support and CuO-Cu₂O /MCA.

Fig. 3(a)-(d) shows the TEM images of CuO-Cu₂O /MCA catalyst. Fig. 3(a) and (b) are the bright field images indicate that the solid phase of the catalyst was mainly composed of the CuO-Cu₂O nanoparticles and interconnected carbon nanoparticles (about 20-30 nm). Large quantities of mesopores of different size were produced among the nanoparticles. The prepared MCA has a three- dimensional network structure and the CuO-Cu₂O nanoparticles successfully embedded and well-dispersed in the amorphous MCA. Fig. 3(c) and (d) present high resolution TEM images of the framed parts in Fig. 3(a) and (b), which displays an obviously crystalline spinel structure of nanocrystals in the catalyst, consisting with XRD patterns showed in Fig. 2. The diameters of 175 grains of CuO-Cu₂O nanoparticles were measured and plotted as the histograms in Fig. 4. It shows that the size distribution of CuO-Cu₂O nanoparticle, mainly ranging from 6 to 14 nm, was obtained with retained monodispersity.

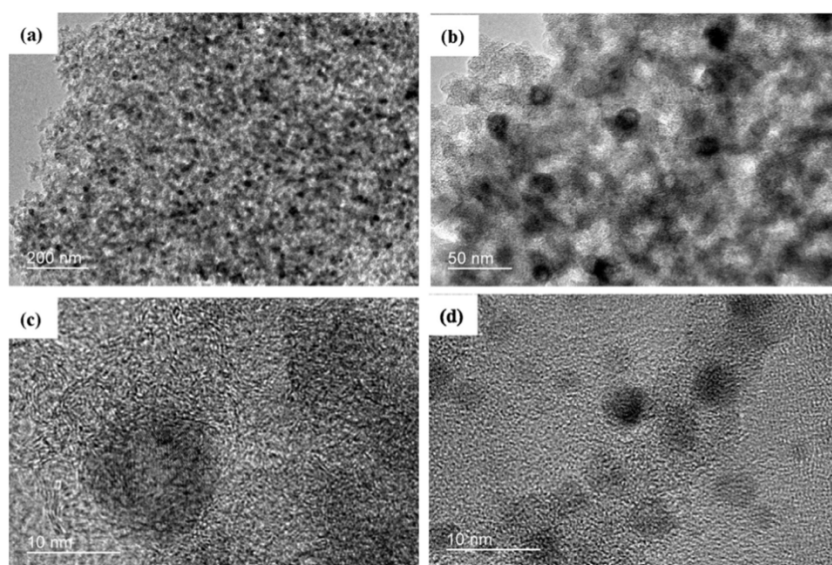


Fig. 3. TEM images of CuO-Cu₂O /MCA catalyst.

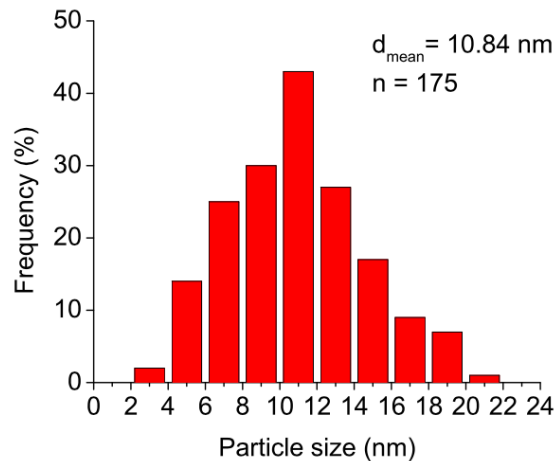


Fig. 4. Particle size distribution of CuO-Cu₂O /MCA catalyst.

3.2. Dye degradation by different treatment processes

COD removal and decolorization ratio in ozonation alone, catalytic ozonation, and pure adsorption by catalyst under the same conditions are shown in Fig. 5. As is observed in Fig. 5(a), COD reduced gradually in either single ozonation or catalytic ozonation as the treatment time lasted to the end. This is because ozone was injected into the reactor continuously, providing sufficient oxidant to degrade dyes in solution. By comparing the catalytic ozonation with ozonation alone, it is noticeable that catalytic ozonation has greater COD reduction than that in ozonation without the catalyst. After 30-min treatment, 28% of initial COD was reduced in catalytic ozonation, which was 10% more than COD removal in ozonation alone. The difference was further enlarged as the treatment pro- longed. The final COD retained only around 54% after the entire catalytic ozonation, while it was nearly 70% in the ozonation process without catalyst. The presence of the novel catalyst significantly improved dye degradation in terms of COD reduction. Considering the COD removal was negligible and irrelevant with treatment time in adsorption, it is clear that the improvement in COD elimination was predominantly attributed to the strengthened degradation of RB-5 in ozonation by the catalyst, rather than its physical adsorption. In addition, catalytic ozonation also shows its advantage in color removal (Fig. 5(b)). Similar to COD reduction, color removal rates in catalytic ozonation are always better than that from single ozonation at each sampling point. The principal mechanism activating the catalytic ozonation is that CuO-Cu₂O / MCA catalyst accelerated the initiation of free radicals derived from the catalytic decomposition of ozone, which possesses higher oxidation potential and

resulted in the enhancement degradation of organic pollutants (Mahmoodi, 2011; Qin et al., 2009).

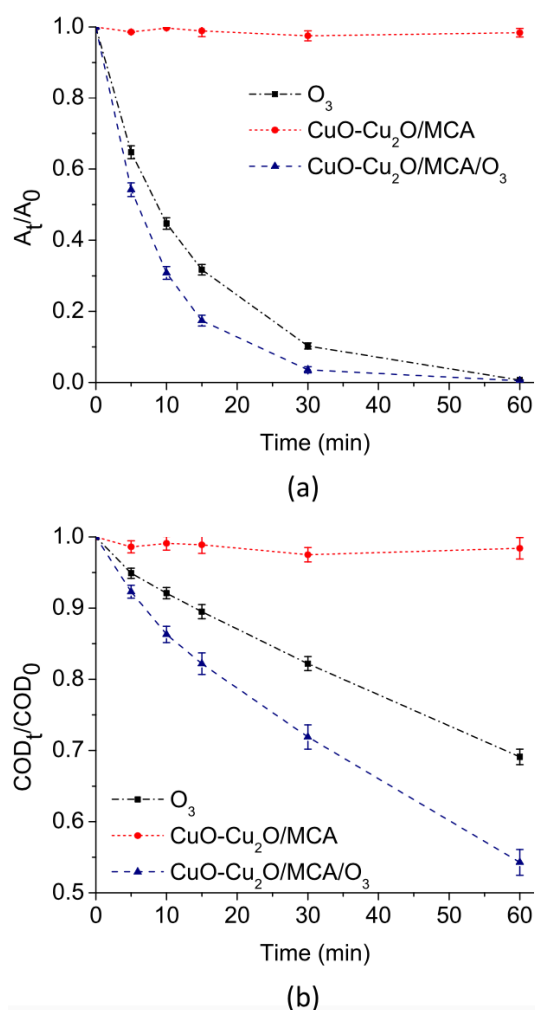


Fig. 5. Comparison of the COD removal (a) and decolorization (b) in different processes. Reaction condition: $T= 30\text{ }^\circ\text{C}$; $pH= 5.1$; ozone dosage= 4.0 mg/min ; catalyst dosage= 1 g ; $C_{initial\text{ }RB-5}= 800\text{ mg/L}$, $COD_{initial}= 625\text{ mg/L}$. The error bars represent the standard deviation of three independent experiments.

Besides, comparing the removal rate of COD in Fig. 5(a) with color in Fig. 5(b), it is found that decolorization was more than 85% after the first 30-min ozonation while the of COD removal rate was no higher than 30%. A reasonable explanation for this result is that the organic pollutants which contribute to color and COD are quite different. The color was predominantly contributed by the dyes possessing complete chromophore, because only these substances have strong absorbance at their maximum absorbance wavelength ($\lambda_{max}= 594\text{ nm}$). Unlike color determination, almost all the organic pollutants, both dyes with complete chromophore and dye fragments, are responsible

for COD. In the very beginning of ozonation, decolorization dominates the degradation reaction, in which the dye chromophore was possibly destructed by cleavage of the -N=N- group in RB-5 (Turhan and Ozturkcan, 2013). This is because cleavage of -N=N- group is much easier than oxidize the dye fragments from decolorization (Zhang et al., 2011), resulting in higher decolorization rate but lower COD removal during ozonation.

3.3. Effect of various parameters on dye degradation

3.3.1. Effect of temperature

Reaction temperature will significantly influence the solubility and stability of ozone in water (Gomes et al., 2010), which may influence the ozonation efficiency. The effect of operational temperature on color and COD removal was evaluated at 30 °C, 45 °C and 60 °C. As is shown in Fig. 6, the result clearly demonstrated that improve the temperature benefited color and COD removal under the specific condition. As temperature was enhanced from 30 °C to 60 °C, the difference of color removal rate were not remarkable, indicating that decolorization of RB-5 in aqueous solution at high temperature is not necessary if consider the energy consumption. The final COD removals were 46%, 50% and 57% when ozonation performed at 30 °C, 45 °C and 60 °C, in which more noticeable improved degradation occurred. In general, improve the temperature will decrease the solubility of ozone and reduce the mass transfer of ozone into aqueous solution, which has adverse impact on dye degradation. However, in the current study both COD and color removal were slightly enhanced. The possible reason for this may be the oxidation rate of ozonation was accelerated significantly although the mass transfer of ozone was depressed.

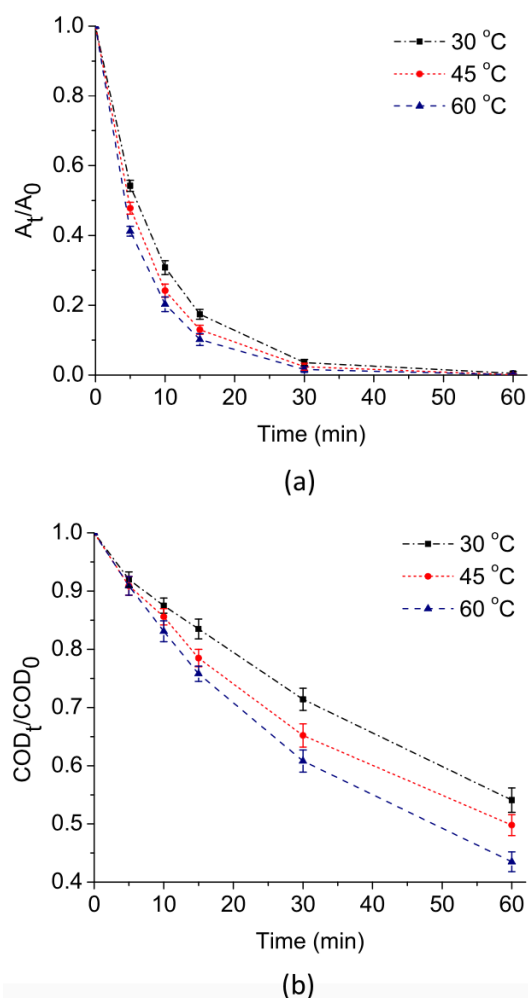


Fig. 6. Effect of temperature on the decolorization (a) and COD removal (b). Reaction condition: pH= 5.1; ozone dosage= 4.0 mg/min; catalyst dosage= 1 g; $C_{initial\ RB-5}$ = 800 mg/L, $COD_{initial}$ = 625 mg/L. The error bars represent the standard deviation of three independent experiments.

3.3.2. Effect of pH

The pH of textile effluent varies to a great extent, the efficiency of ozonation and the degradation pathways of dye may be affected by solution pH. Hence it is necessary to understand the effect of pH on the color and COD removal in catalytic ozonation. The effect of applied solution pH on dye decomposition was examined in 4 different experiments, in which the solution pH was 3.5, 5.1, 7.8 and 10.6. According to Fig. 7, the color and COD removal of RB-5 in strong alkaline aqueous (pH=10.6) solution was the greater than those in weak alkaline (pH=7.8) or acidic conditions (pH=5.1 and pH=3.5). The 57% COD removal was obtained at pH= 10.6 after 1 h catalytic ozonation. The phenomenon was caused by the following factors: (a) the ozone decomposition

will be greatly enhanced under alkaline condition to generate $\cdot\text{OH}$ (Zhang et al., 2011) and the highly reactive radicals will greatly increase the reaction process (Chiou et al., 2013). The dye organic compounds therefore can be decomposed more effectively; (b) the dye solution pH also affects the surface characteristics of the catalyst, particularly the surface charge which has important effect on their adsorption capacity towards organic dye molecules and the intermediate products (Dobson et al., 1997; Szekeres and Tombacz, 2012).

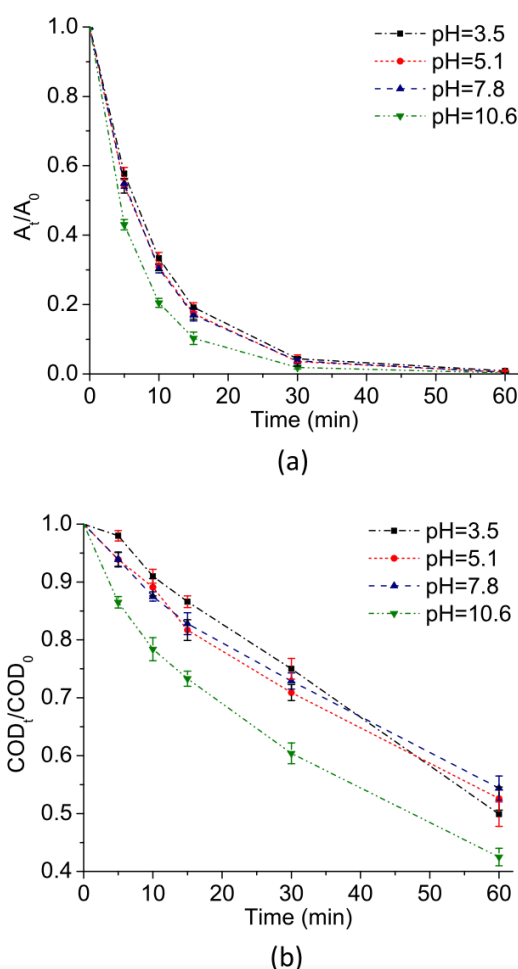


Fig. 7. Effect of pH on the decolorization (a) and COD removal (b). Reaction condition: $T = 30\text{ }^\circ\text{C}$; ozone dosage = 4.0 mg/min; catalyst dosage = 1 g; $C_{\text{initial RB-5}} = 800\text{ mg/L}$, $\text{COD}_{\text{initial}} = 625\text{ mg/L}$. The error bars represent the standard deviation of three independent experiments.

3.3.3. Effect of ozone dosage

The effect of ozone dosage is shown in Fig. 8. The ozone concentration of inlet gas was set to 8 mg/L, and the gas flow was fixed at 250, 500 and 1000 mL/min in three runs.

It is clearly that the color and COD removal rates were significantly affected by the inlet ozone dosage. According to Fig. 8(b), the COD removal enhanced from 35% to 57% after 60-min ozonation when the inlet ozone dosage increased from 2 to 8 mg/min. A possible explanation for this enhancement efficiency is that the mass transfer driving force was enhanced and ozone-derived free radicals (such as $\cdot\text{OH}$) was generated when ozone concentration in the dye solution was boomed by increased supplying gas flowrate (Moslemi et al., 2010). The phenomenon is at good agreement with a previously study regarding decomposition of C. I. Basic Blue 9 by ozonation with granular activated carbon (Gholami-Borujeni et al., 2013).

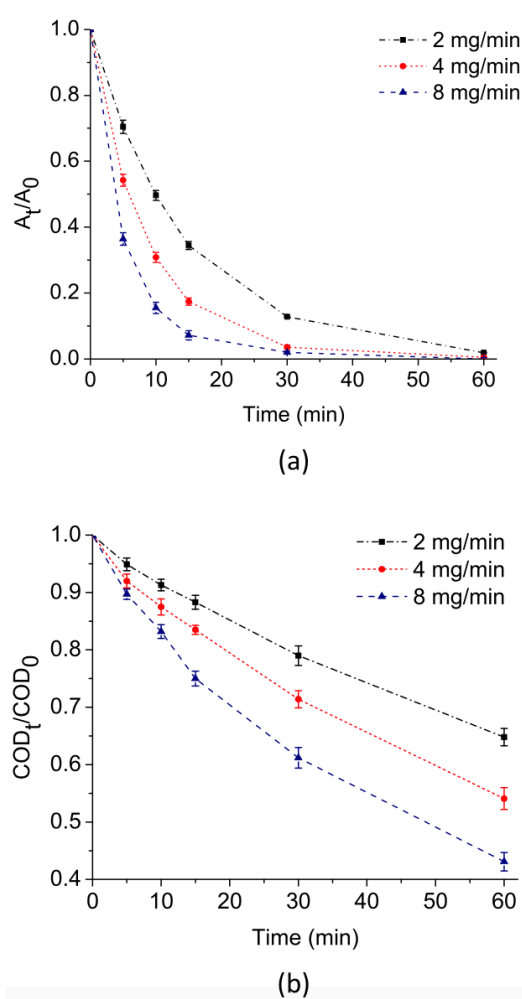


Fig. 8. Effect of ozone dosage on the decolorization (a) and COD removal (b). Reaction condition: $T= 30\text{ }^\circ\text{C}$; $\text{pH}= 5.1$; catalyst dosage= 1 g; $C_{\text{initial } RB-5} = 800\text{ mg/L}$, $\text{COD}_{\text{initial}} = 625\text{ mg/L}$. The error bars represent the standard deviation of three independent experiments.

3.3.4. Effect of amount of the catalyst

Fig. 9 presents the effect of catalyst dosage on dye degradation. Experiments were performed at various amounts of catalyst, 0.5, 1.0 and 3.0 g. According to Fig. 9(a), the effect of catalyst loading has minimal influence on color removal, although catalytic ozonation displayed better decolorization performance than ozonation alone without catalyst. This finding probably suggested that decolorization did not require too much catalyst in the reaction system. At current ozonation condition, 1.0 g of catalyst was excessive for decoloration of RB-5 solution. Fig. 9(b) shows the evolution of COD during catalytic ozonation with various catalyst dosages. As is expected, COD reduced more significantly when the amount of CuO-Cu₂O /MCA catalyst was raised to 3.0 g. Its reduction rate, after 60-min treatment, was enhanced by 21% of the original COD when comparing to the process with only 0.5 g of the catalyst. The possible reasons may be attributed to the expansion of contact surface area and availability of reactive sites of the catalyst when the catalyst amount was raised (Shahamat et al., 2014). The enlarged contact surface area hence facilitated reaction between ozone and the pollutants (Bhatnagar et al., 2013), and the growing reactive sites effectively promoted ozone decomposition to generate reactive radicals for dye degradation (Lei et al., 2007).

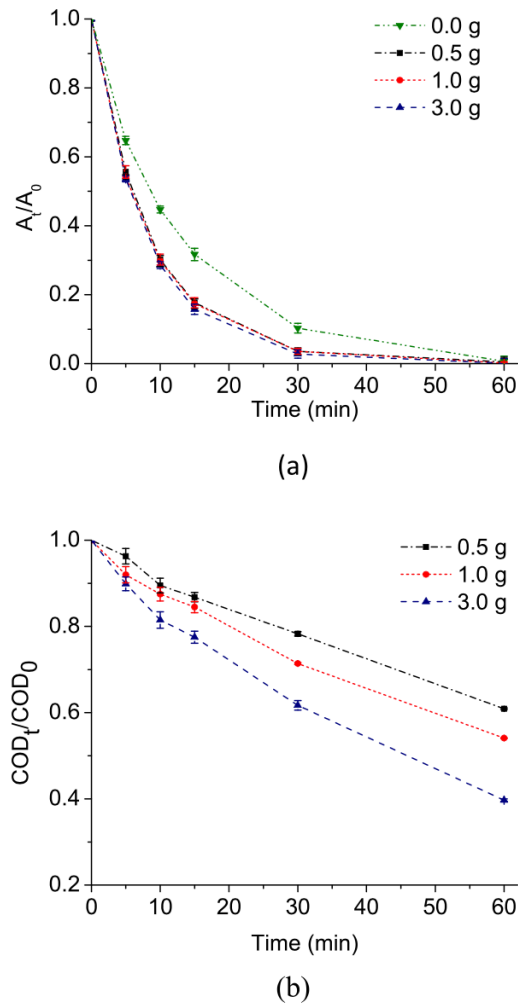


Fig. 9. Effect of catalyst amount on the decolorization (a) and COD removal (b). Reaction condition: $T=30\text{ }^{\circ}\text{C}$; $\text{pH}=5.1$; Ozone dosage= 4.0 mg/min ; $C_{initial\text{ RB-5}}=800\text{ mg/L}$, $COD_{initial}=625\text{ mg/L}$. The error bars represent the standard deviation of three independent experiments.

3.3.5. Effect of applied dye concentration

The influence of applied RB-5 concentration on color and COD removal rate was also explored with different applied concentration from 400 to 1600 mg/L. As is illustrated in Fig. 10(a), the dye decolorization and COD removal changed inversely to the applied concentration of RB-5. Higher color and COD removal rate was much easier to obtain in the process which adopted dye solution of relative lower initial concentration. For an instance, it only required 10 min to achieve 80% decolorization in the treatment adopting 400 mg/L dye solution, while an extra 5-min ozonation is necessary to accomplish the same decolorization requirement in the process when the dye solution

of doubled concentration, 800 mg/L, was applied. The possible explanation might be that the ratios of ozone molecules to dye molecules in the solution decreased when more concentrated dye solution was used (Tehrani-Bagha et al., 2010), leading to a growing excess of dye regarding to ozone in decolorization. As a result, the decolorization and COD elimination for the high initial dye concentrations required longer time than the lower dye concentration.

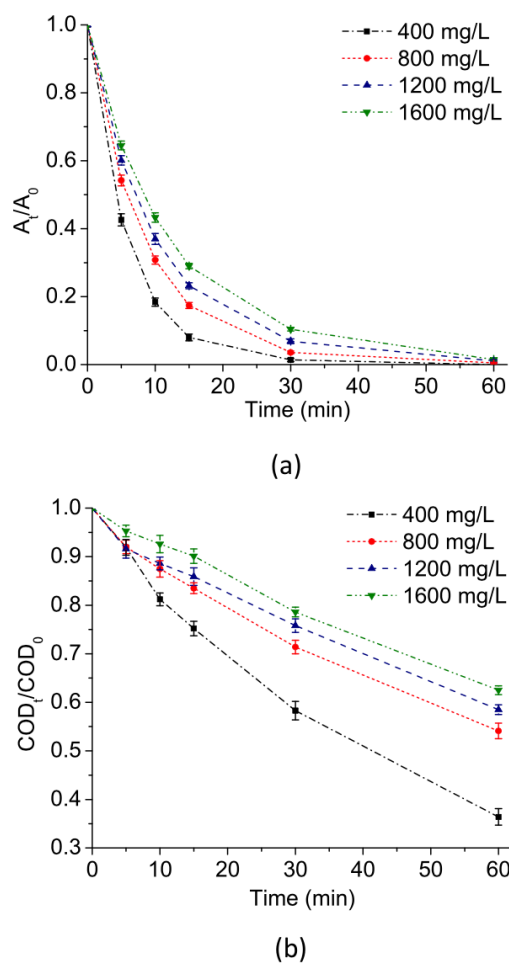


Fig. 10. Effect of dye concentration on the decolorization (a) and COD removal (b). Reaction condition: $T=30\text{ }^\circ\text{C}$; $\text{pH}=5.1$; Ozone dosage= 4.0 mg/min ; $C_{initial\text{ RB-5}}=800\text{ mg/L}$, $COD_{initial}=625\text{ mg/L}$. The error bars represent the standard deviation of three independent experiments.

3.4. Investigation on decolorization process

The time dependent UV-Vis spectrum of RB-5 solution during catalytic ozonation is exhibited in Fig. 11. RB-5 has a maximum absorbance at the wavelength of 594 nm in

the visible region and two other absorption peaks at 307 and 388 nm in the UV region. The absorption peak was weakened as the ozonation progressed, and the absorption peak at $\lambda_{\max}= 594$ nm almost diminished at the end of the treatment. The absorbance in the visible region belongs to azo group and those in the UV region relates to both aryl and naphthalene-like moieties (Lucas et al., 2006). The decreases in intensity of the absorption peaks in visible region suggest that $-N=N-$ group in RB-5, which is responsible for color, was possibly cleaved by ozone or its derived reactive species (Turhan and Ozturkcan, 2013). Another phenomenon worth noting is that the reduction of maximum absorbance in the visible region was rapider than those in UV region. After 60 min treatment the absorbance in visible region almost completely disappeared. This indicated the azo structure in dye molecule, which act as dye chromophore, were easy to be destructed in ozonation. Nevertheless, the absorbance in the UV region was still moderate when ozonation completed. This suggested that there were still a certain amount of aromatic rings in dye solution were not mineralized into inorganics, which tended to be more difficult to oxidize than azo structure in ozonation. This finding is at good agreement with the results presents in Fig. 5, in which total decolorization was accomplished, while COD, contributed partially by aromatic rings, still retained in dye solution at moderate level.

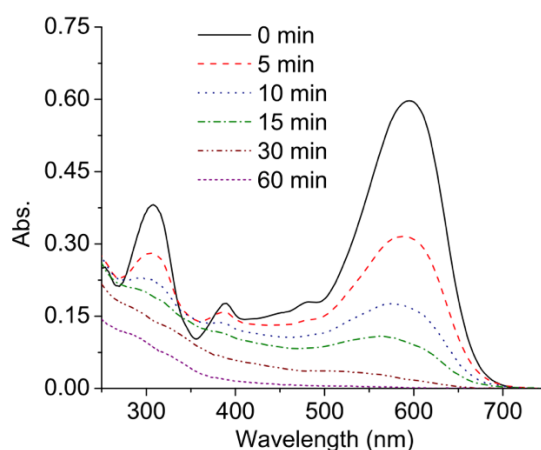


Fig. 11. Evolution of UV-Vis spectral of RB-5 solution during catalytic ozonation. Reaction condition: $T= 30$ °C; $pH= 5.1$; Ozone dosage= 4.0 mg/min; $C_{initial\ RB-5}= 800$ mg/L, $COD_{initial}= 625$ mg/L.

4. Conclusions

The novel CuO-Cu₂O /MCA catalyst was successfully prepared by coupling sol-gel process with impregnation method. The characterization results demonstrated that the CuO-Cu₂O nano- particles successfully embedded and well-dispersed in the amorphous MCA, and the particle size retained monodispersity ranging from 6 to 14 nm mainly. In catalytic ozonation with the novel catalyst, the study clearly shows that degradation of the RB-5 dye in aqueous solution was notably promoted comparing with ozonation in the absence of the catalyst. The COD removal was enhanced to 46% whereas it was only 29% in non-catalytic ozonation after 60- min treatment. This leads to a conclusion that the CuO-Cu₂O / MCA was a highly efficient catalyst for catalytic degradation of synthetic dye with ozone. In the investigation of experiment variables, it shows that increasing the reaction temperature, pH, ozone dosage or catalyst loading led to enhanced dye degradation in terms of decolorization and COD reduction, especially for the latter. The UV-Vis spectrum suggested chromophoric group was easier to be destructed in ozonation comparing with aromatic structure. To conclude, the novel catalyst could be potentially used in catalytic ozonation for dyeing wastewater treatment.

References

1. Abidi, N., Errais, E., Duplay, J., Berez, A., Jrad, A., Schaefer, G., Ghazi, M., Semhi, K., Trabelsi-Ayadi, M., 2015. Treatment of dye-containing effluent by natural clay. *J. Clean. Prod.* 86, 432e440. <http://dx.doi.org/10.1016/j.jclepro.2014.08.043>.
2. Asghar, A., Abdul Raman, A.A., Wan Daud, W.M.A., 2015. Advanced oxidation processes for in-situ production of hydrogen peroxide/hydroxyl radical for textile wastewater treatment: a review. *J. Clean. Prod.* 87, 826e838. <http://dx.doi.org/10.1016/j.jclepro.2014.09.010>.
3. Beltran, F.J., Rivas, F.J., Montero-de-Espinosa, R., 2005. Iron type catalysts for the ozonation of oxalic acid in water. *Water Res.* 39, 3553e3564. <http://dx.doi.org/10.1016/j.watres.2005.06.018>.

4. Bhatnagar, A., Hogland, W., Marques, M., Sillanpaa, M., 2013. An overview of the modification methods of activated carbon for its water treatment applications. *Chem. Eng. J.* 219, 499e511. <http://dx.doi.org/10.1016/j.cej.2012.12.038>.
5. Bootharaju, M.S., Pradeep, T., 2013. Facile and rapid synthesis of a dithiol-protected Ag₇ quantum cluster for selective adsorption of cationic dyes. *Langmuir: ACS J. Surf. Colloids* 29, 8125e8132. <http://dx.doi.org/10.1021/la401180r>.
6. Chiou, C.S., Chuang, K.J., Lin, Y.F., Chen, H.W., Ma, C.M., 2013. Application of ozone related processes to mineralize tetramethyl ammonium hydroxide in aqueous solution. *Int. J. Photoenergy* 2013, 1e7. <http://dx.doi.org/10.1155/2013/191742>.
7. Ciccotti, L., do Vale, L.A.S., Hower, T.L.R., Freire, R.S., 2015. Fe₃O₄@TiO₂ preparation and catalytic activity in heterogeneous photocatalytic and ozonation processes. *Catal. Sci. Technol.* 5, 1143e1152. <http://dx.doi.org/10.1039/C4cy01242a>.
8. Dobson, K.D., Connor, P.A., Mcquillan, A.J., 1997. Monitoring hydrous metal oxide surface charge and adsorption by STIRS. *Langmuir* 13, 2614e2616. <http://dx.doi.org/10.1021/la961053q>.
9. Fanchiang, J.M., Tseng, D.H., 2009. Degradation of anthraquinone dye C.I. Reactive Blue 19 in aqueous solution by ozonation. *Chemosphere* 77, 214e221. <http://dx.doi.org/10.1016/j.chemosphere.2009.07.038>.
10. Gharbani, P., Mehrizad, A., 2014. Heterogeneous catalytic ozonation process for removal of 4-chloro-2-nitrophenol from aqueous solutions. *J. Saudi Chem. Soc.* 18, 601e605. <http://dx.doi.org/10.1016/j.jscs.2012.07.013>.
11. Gholami-Borujeni, F., Naddafi, K., Nejat-zade-Barandozi, F., 2013. Application of catalytic ozonation in treatment of dye from aquatic solutions. *Desalin. Water Treat.* 51, 6545e6551. <http://dx.doi.org/10.1080/19443994.2013.769491>.
12. Gomes, A.C., Nunes, J.C., Simoes, R.M., 2010. Determination of fast ozone oxidation rate for textile dyes by using a continuous quench-flow system. *J. Hazard. Mater.* 178, 57e65. <http://dx.doi.org/10.1016/j.jhazmat.2010.01.043>.
13. Gomez, S., Marchena, C.L., Renzini, M.S., Pizzio, L., Pierella, L., 2015. In situ generated TiO₂ over zeolitic supports as reusable photocatalysts for the degradation of dichlorvos. *Appl. Catal. B Environ.* 162, 167e173. <http://dx.doi.org/10.1016/j.apcatb.2014.06.047>.

14. He, Y.Z., Wang, X.J., Xu, J.L., Yan, J.L., Ge, Q.L., Gu, X.Y., Jian, L., 2013. Application of integrated ozone biological aerated filters and membrane filtration in water reuse of textile effluents. *Bioresour. Technol.* 133, 150e157. <http://dx.doi.org/10.1016/j.biortech.2013.01.074>.
15. Lei, L., Gu, L., Zhang, X., Su, Y., 2007. Catalytic oxidation of highly concentrated real industrial wastewater by integrated ozone and activated carbon. *Appl. Catal. A Gen.* 327, 287e294. <http://dx.doi.org/10.1016/j.apcata.2007.05.027>.
16. Lin, Y.F., Chang, C.Y., 2014. Magnetic mesoporous iron oxide/carbon aerogel photocatalysts with adsorption ability for organic dye removal. *Rsc Adv.* 4, 28628e28631. <http://dx.doi.org/10.1039/C4ra03436h>.
17. Liu, R.L., Wan, L., Liu, S.Q., Pan, L.X., Wu, D.Q., Zhao, D.Y., 2015a. An interface-induced co-assembly approach towards ordered mesoporous carbon/graphene aerogel for high-performance supercapacitors. *Adv. Funct. Mater.* 25, 526e533. <http://dx.doi.org/10.1002/adfm.201403280>.
18. Liu, W.W., Li, X., Zhu, M.H., He, X., 2015b. High-performance all-solid state asymmetric supercapacitor based on Co₃O₄ nanowires and carbon aerogel. *J. Power Sources* 282, 179e186. <http://dx.doi.org/10.1016/j.jpowsour.2015.02.047>.
19. Lucas, M.S., Amaral, C., Sampaio, A., Peres, J.A., Dias, A.A., 2006. Biodegradation of the diazo dye Reactive Black 5 by a wild isolate of *Candida oleophila*. *Enzym. Microb. Technol.* 39, 51e55. <http://dx.doi.org/10.1016/j.enzmictec.2005.09.004>.
20. Mahmoodi, N.M., 2011. Photocatalytic ozonation of dyes using copper ferrite nanoparticle prepared by co-precipitation method. *Desalination* 279, 332e337. <http://dx.doi.org/10.1016/j.desal.2011.06.027>.
21. Mahmoodi, N.M., 2013. Photocatalytic ozonation of dyes using multiwalled carbon nanotube. *J. Mol. Catal. A Chem.* 366, 254e260. <http://dx.doi.org/10.1016/j.molcata.2012.10.002>.
22. Mehrjouei, M., Muller, S., Moller, D., 2014. Energy consumption of three different advanced oxidation methods for water treatment: a cost-effectiveness study. *J. Clean. Prod.* 65, 178e183. <http://dx.doi.org/10.1016/j.jclepro.2013.07.036>.
23. Moslemi, M., Davies, S.H., Masten, S.J., 2010. Ozone mass transfer in a recirculating loop semibatch reactor operated at high pressure. *J. Adv. Oxid. Technol.* 13, 79e88.

24. Ozturk, E., Karaboyaci, M., Yetis, U., Yigit, N.O., Kitis, M., 2015. Evaluation of integrated pollution prevention control in a textile fiber production and dyeing mill. *J. Clean. Prod.* 88, 116e124. <http://dx.doi.org/10.1016/j.jclepro.2014.04.064>.
25. Park, H.W., Kim, J.K., Hong, U.G., Lee, Y.J., Song, J.H., Song, I.K., 2013. Catalytic decomposition of 4-phenoxyphenol over Pd/XCs_{2.5}H_{0.5}PW₁₂O₄₀/ACA (activated carbon aerogel)-SO₃H (X 1/4 10e30 wt%) catalysts. *Appl. Catal. A Gen.* 453, 287e294. <http://dx.doi.org/10.1016/j.apcata.2012.12.037>.
26. Peng, L., Dong, S.Y., Li, N., Suo, G.C., Huang, T.L., 2015. Construction of a biocompatible system of hemoglobin based on AuNPs-carbon aerogel and ionic liquid for amperometric biosensor. *Sens. Actuat. B Chem.* 210, 418e424. <http://dx.doi.org/10.1016/j.snb.2014.12.122>.
27. Petre, A.L., Carbajo, J.B., Rosal, R., Garcia-Calvo, E., Perdigon-Melon, J.A., 2013. CuO/ SBA-15 catalyst for the catalytic ozonation of mesoxalic and oxalic acids. Water matrix effects. *Chem. Eng. J.* 225, 164e173. <http://dx.doi.org/10.1016/j.cej.2013.03.071>.
28. Qiang, Z., Ling, W., Tian, F., 2013. Kinetics and mechanism for omethoate degradation by catalytic ozonation with Fe(III)-loaded activated carbon in water. *Chemosphere* 90, 1966e1972. <http://dx.doi.org/10.1016/j.chemosphere.2012.10.059>.
29. Qin, W., Li, X., Qi, J.Y., 2009. Experimental and theoretical investigation of the catalytic ozonation on the surface of NiO-CuO nanoparticles. *Langmuir: ACS J. Surf. Colloids* 25, 8001e8011. <http://dx.doi.org/10.1021/La900476m>.
30. Qu, R.J., Xu, B.Z., Meng, L.J., Wang, L.S., Wang, Z.Y., 2015. Ozonation of indigo enhanced by carboxylated carbon nanotubes: performance optimization, degradation products, catalytic mechanism and toxicity evaluation (vol. 68. pg 316, 2014). *Water Res.* 70, 495. <http://dx.doi.org/10.1016/j.watres.2014.12.045>.
31. Ramachandran, G., Kumarasamy, T., 2013. Degradation of textile dyeing wastewater by a modified solar photo-fenton process using steel scrap/H₂O₂. *Clean Soil Air Water* 41, 267e274. <http://dx.doi.org/10.1002/clen.201100462>.
32. Rosa, J.M., Fileti, A.M.F., Tambourgi, E.B., Santana, J.C.C., 2015. Dyeing of cotton with reactive dyestuffs: the continuous reuse of textile wastewater effluent

- treated by ultraviolet/hydrogen peroxide homogeneous photocatalysis. *J. Clean. Prod.* 90, 60e65. <http://dx.doi.org/10.1016/j.jclepro.2014.11.043>.
33. Saroj, S., Kumar, K., Pareek, N., Prasad, R., Singh, R.P., 2014. Biodegradation of azo dyes acid red 183, direct blue 15 and direct red 75 by the isolate *Penicillium oxalicum* SAR-3. *Chemosphere* 107, 240e248. <http://dx.doi.org/10.1016/j.chemosphere.2013.12.049>.
 34. Shahamat, Y.D., Farzadkia, M., Nasserli, S., Mahvi, A.H., Gholami, M., Esrafil, A., 2014. Magnetic heterogeneous catalytic ozonation: a new removal method for phenol in industrial wastewater. *J. Environ. Health Sci.* 12 <http://dx.doi.org/10.1186/2052-336x-12-50>.
 35. Sun, H., Xu, Z., Gao, C., 2013a. Multifunctional, ultra-flyweight, synergistically assembled carbon aerogels. *Adv. Mater.* 25, 2554e2560. <http://dx.doi.org/10.1002/adma.201204576>.
 36. Sun, J., Yan, X., Lv, K., Sun, S., Deng, K., Du, D., 2013b. Photocatalytic degradation pathway for azo dye in $\text{TiO}_2/\text{UV}/\text{O}_3$ system: hydroxyl radical versus hole. *J. Mol. Catal. A Chem.* 367, 31e37. <http://dx.doi.org/10.1016/j.molcata.2012.10.020>.
 37. Szekeres, M., Tombacz, E., 2012. Surface charge characterization of metal oxides by potentiometric acid-base titration, revisited theory and experiment. *Colloid Surf. A* 414, 302e313. <http://dx.doi.org/10.1016/j.colsurfa.2012.08.027>.
 38. Tehrani-Bagha, A.R., Mahmoodi, N.M., Menger, F.M., 2010. Degradation of a persistent organic dye from colored textile wastewater by ozonation. *Desalination* 260, 34e38. <http://dx.doi.org/10.1016/j.desal.2010.05.004>.
 39. Tian, S., Zhang, J., Chen, J., Kong, L., Lu, J., Ding, F., Xiong, Y., 2013. $\text{Fe}_2(\text{MoO}_4)_3$ as an effective photo-fenton-like catalyst for the degradation of anionic and cationic dyes in a wide pH range. *Ind. Eng. Chem. Res.* 52, 13333e13341. <http://dx.doi.org/10.1021/ie401522a>.
 40. Turhan, K., Ozturkcan, S.A., 2013. Decolorization and degradation of reactive dye in aqueous solution by ozonation in a semi-batch bubble column reactor. *Water Air Soil Pollut.* 224 <http://dx.doi.org/10.1007/S11270-012-1353-8>.
 41. Turkay, O., Man, H., Dimoglo, A., 2014. Experimental and theoretical investigations of CuO-catalyzed ozonation of humic acid. *Sep. Purif. Technol.* 134, 110e116. <http://dx.doi.org/10.1016/j.seppur.2014.07.040>.

42. Udrea, I., Bradu, C., 2003. Ozonation of substituted phenols in aqueous solutions over CuO-Al₂O₃ catalyst. *Ozone Sci. Eng.* 25, 335e343. <http://dx.doi.org/10.1080/01919510390481658>.
43. Vacchi, F.I., Albuquerque, A.F., Vendemiatti, J.A., Morales, D.A., Ormond, A.B., Freeman, H.S., Zocolo, G.J., Zanoni, M.V.B., Umbuzeiro, G., 2013. Chlorine disinfection of dye wastewater: implications for a commercial azo dye mixture. *Sci. Total Environ.* 442, 302e309. <http://dx.doi.org/10.1016/j.scitotenv.2012.10.019>.
44. Vijayalakshmi, P., Raju, G.B., Gnanamani, A., 2011. Advanced oxidation and electrooxidation as tertiary treatment techniques to improve the purity of tannery wastewater. *Ind. Eng. Chem. Res.* 50, 10194e10200. <http://dx.doi.org/10.1021/Ie201039z>.
45. Wang, B., Karthikeyan, R., Lu, X.Y., Xuan, J., Leung, M.K.H., 2013a. High photo-catalytic activity of immobilized TiO₂ nanorods on carbonized cotton fibers. *J. Hazard. Mater.* 263, 659e669. <http://dx.doi.org/10.1016/j.jhazmat.2013.10.029>.
46. Wang, H.X., Zhang, W., Zhao, J.X., Xu, L.L., Zhou, C.Y., Chang, L., Wang, L.Y., 2013b. Rapid decolorization of phenolic azo dyes by immobilized laccase with Fe₃O₄/SiO₂ nanoparticles as support. *Ind. Eng. Chem. Res.* 52, 4401e4407. <http://dx.doi.org/10.1021/Ie302627c>.
47. Woan, K., Pyrgiotakis, G., Sigmund, W., 2009. Photocatalytic carbon-nanotube-TiO₂ composites. *Adv. Mater.* 21, 2233e2239. <http://dx.doi.org/10.1002/adma.200802738>.
48. Wu, X., Wu, D., Fu, R., 2007. Studies on the adsorption of reactive brilliant red X-3B dye on organic and carbon aerogels. *J. Hazard. Mater.* 147, 1028e1036. <http://dx.doi.org/10.1016/j.jhazmat.2007.01.139>.
49. Wu, X., Yang, X., Wu, D., Fu, R., 2008. Feasibility study of using carbon aerogel as particle electrodes for decoloration of RBRX dye solution in a three-dimensional electrode reactor. *Chem. Eng. J.* 138, 47e54. <http://dx.doi.org/10.1016/j.cej.2007.05.027>.
50. Wu, X.B., Hui, K.N., Hui, K.S., Lee, S.K., Zhou, W., Chen, R., Hwang, D.H., Cho, Y.R., Son, Y.G., 2012. Adsorption of basic yellow 87 from aqueous solution onto two different mesoporous adsorbents. *Chem. Eng. J.* 180, 91e98. <http://dx.doi.org/10.1016/j.cej.2011.11.009>.

51. Yang, Y.X., Ma, J., Qin, Q.D., Zhai, X.D., 2007. Degradation of nitrobenzene by nano- TiO_2 catalyzed ozonation. *J. Mol. Catal. A Chem.* 267, 41e48. <http://dx.doi.org/10.1016/j.molcata.2006.09.010>.
52. Yıldırım, A.O., Gül, S., Eren, O., Kusyuran, E., 2011. A comparative study of ozonation, homogeneous catalytic ozonation, and photocatalytic ozonation for C.I. reactive red 194 azo dye degradation. *Clean Soil Air Water* 39, 795e805. <http://dx.doi.org/10.1002/clen.201000192>.
53. Yin, L.W., Zhang, Z.W., Li, Z.Q., Hao, F.B., Li, Q., Wang, C.X., Fan, R.H., Qi, Y.X., 2014. Spinel ZnMn_2O_4 nanocrystal-anchored 3D hierarchical carbon aerogel hybrids as anode materials for lithium ion batteries. *Adv. Funct. Mater.* 24, 4176e4185. <http://dx.doi.org/10.1002/adfm.201400108>.
54. Zhang, X.Y., Li, X., Qin, W., 2009. Investigation of the catalytic activity for ozonation on the surface of NiO nanoparticles. *Chem. Phys. Lett.* 479, 310e315. <http://dx.doi.org/10.1016/j.cplett.2009.08.029>.
55. Zhang, T., Li, W.W., Croue, J.P., 2011. Catalytic ozonation of oxalate with a cerium supported palladium oxide: an efficient degradation not relying on hydroxyl radical oxidation. *Environ. Sci. Technol.* 45, 9339e9346. <http://dx.doi.org/10.1021/Es202209j>.
56. Zhang, Y.N., Jin, Y.F., Huang, X.F., Shi, H.J., Zhao, G.H., Zhao, H.Y., 2014. Nano-crystalline TiO_2 /carbon aerogel electrode with high surface area and enhanced photoelectrocatalytic oxidation capacity. *Electrochim. Acta* 130, 194e199. <http://dx.doi.org/10.1016/j.electacta.2014.03.010>.
57. Zhao, H., Dong, Y.M., Jiang, P.P., Wang, G.L., Zhang, J.J., Li, K., Feng, C.Y., 2014. An alpha- MnO_2 nanotube used as a novel catalyst in ozonation: performance and the mechanism. *New J. Chem.* 38, 1743e1750. <http://dx.doi.org/10.1039/C3nj01523h>.